Photoelastic evaluation of fiber surface-treatments on the interfacial performance of a polyester fiber/epoxy model composite

E.A. Flores-Johnson[1], *J.M. Vázquez-Rodríguez*[2], *P.J. Herrera-Franco*[3], *P.I. González-Chi*[3,*]

[1]Institute of Materials Engineering, Australian Nuclear Science and Technology Organisation
Locked Bag 2001, Kirrawee DC, NSW 2232, Australia

[2]Universidad Juárez Autónoma de Tabasco, Av. Universidad S/N Zona de la Cultura CP. 86000
Villahermosa, Tabasco, México

[3]Centro de Investigación Científica de Yucatán, A.C., Unidad de Materiales
Calle 43, No. 130, col. Chuburná de Hidalgo 97200, Mérida, Yucatán, México

Abstract: The interfacial adhesion between a polyester fiber and an epoxy matrix was improved by chemical and topological modifications of the fiber surface. The maximum interfacial shear strength was measured using photoelasticity to assess the interfacial performance in pull-out single-fiber composite specimens. An increase of the interfacial shear strength was observed when plasma-treated or surface-modified fibers were used; also, as the applied load to the free fiber was increased, the fiber treatment caused a reduction of the debonded area at the fiber-matrix interface.

Keywords: Fiber/matrix bond; Optical properties/techniques; Stress transfer; Photoelasticity.

[*]Corresponding author, Email: ivan@cicy.mx; Tel/fax: (+52 999) 9428330/(+52 999) 9813900

1. Introduction

Traditional thermoset composites are reinforced with engineering fibers such as carbon or glass fibers. These composites are well-known by their high strength; nevertheless, due to the brittleness of the reinforcement, they have low toughness. An alternative solution for this problem may be the use of thermoplastic fibers that possess higher toughness when compared to carbon or glass fibers; however, the use of thermoplastic fibers as reinforcement leads to a different problem: their low compatibility to thermosetting matrices produces a weak fiber-matrix interface.

Fiber surface modification by exposure to certain plasma treatments has been used to improve the interfacial adhesion between thermoplastic fibers and a thermosetting matrix; for example, plasma polymerization of a monomer onto the fiber surface produces a thin polymer film firmly attached to the fiber substrate [1]. The functional groups on the surface of the film act as a coupling agent leading to a stronger interfacial bonding between treated fibers and matrix, providing an effective load transfer. Gonzalez-Chi and Young [2] reported an improved interfacial performance of plasma treated polyethylene (PE) fiber/epoxy composites when compared with untreated PE fiber. Wu *et al*. [3] reported an increase of 37.5 % of the interfacial strength of a poly-p-phenylenebenzobizoxazole (PBO)/epoxy composite when the reinforcing fibers where treated with an oxygen plasma process.

Topographical surface modification of the reinforcing fiber has also been used to improve the interfacial adhesion in a composite. A study of the fiber-matrix bond strength of a henequen fiber/high density polyethylene (HDPE) matrix system by Valadez-Gonzalez *et al*. [4] showed that alkali treated fibers had higher roughness than untreated fibers leading to a better fiber-matrix mechanical interlocking, which is the result of interpenetration of the matrix in the fiber surface irregularities. These surface irregularities act as mechanical anchors, leading to a high bond strength even though other interactions may be weak [5]. Sreekumar *et al.* [6] investigated the effect of chemical-treated sisal fibers on the interfacial bonding of polyester (PET) matrix composites. They found that the interfacial bonding between the fibers and the matrix was improved as a result of a rougher fiber surface when compared with untreated fibers. Ou *et al.* [7] studied the effect of grafted Kevlar fibers on the mechanical properties of Kevlar/wood-flour/HDPE composites. They grafted silane and allyl groups onto Kevlar fibers and found that the tensile, flexural and impact properties were improved when compared with non-modified fiber reinforced composites.

Although there are several methods to study the interfacial adhesion in composite materials, the pull-out and single-fiber fragmentation tests are the most commonly used [8, 9]. The pull-out test has been used to study the performance of thermoplastic fiber/thermoset matrix systems: PBO/epoxy [10], PE/epoxy [2], polyester (PET)/epoxy [11].

Photoelasticity is a well-known technique that has been successfully used to experimentally measure the stress fields and the debonding process at a fiber-matrix interface [12, 13]. The photoelastic technique allows the observation of the stress

distribution and the identification of micromechanical events [14]. It also allows the *in situ* analysis of the loading-deformation process of a specimen. Vazquez-Rodriguez *et al.* [11] studied the interface of PET/epoxy composites using photoelasticity and pull-out test; they obtained the interfacial shear stress distribution directly from the image of isochromatic fringes. Zhao *et al*. [15] investigated the interfacial behavior of a plasma-treated glass fiber/epoxy system using photoelasticity and single-fiber composite specimens.

The present paper studies the effect of the surface modification of a polyester fiber on the performance of the fiber-matrix adhesion in a thermoset-based model composite using the pull-out test and photoelasticity. Polyester fibers were treated with a nitrogen-aniline plasma to improve the chemical bonding between the fiber and the matrix. In addition, the surface fiber was physically modified using a SiC abrasive paper to increase the fiber-matrix mechanical interlocking. The interfacial performance of the untreated fiber composites is compared with the plasma-treated and the surface-modified fiber composites.

2. Materials and methods

2.1 Epoxy resin

The resin used as the matrix of the model composites was bisphenol-A epoxy resin DER 331 (supplied by DOW Chemical) and a modified aliphatic amine, Ancamine 1784, was used as curing agent (supplied by Air Products and Chemicals). The stoichiometric relation used was of 0.6 mol of resin/mol of curing agent, which resulted in a plasticized matrix because of the curing agent excess. The curing process of the resin was performed at room temperature under controlled humidity for twenty-one days.

2.2 Fibers

Two types of thermoplastic polyester fibers were used, both with a diameter of D = 1.3 mm and supplied by Kirschbaum: untreated (UT) fiber and textured fiber (TX).

The tensile properties of the fibers were measured according to ASTM D2343-67 standard using a universal testing machine (Shimatzu AG1) fit with a 5 kN load cell. The test was performed with a cross-head speed of 30 mm/min and a gauge length of 245 mm.

2.3 Surface modification of fibers

UT fibers were topographically modified to improve the mechanical bonding (interlocking) between the fiber and the matrix. This surface modification was achieved by sanding the fiber surface with 2000 grit SiC abrasive paper, and then these surface-modified (SM) fibers were washed with xylene.

The UT fibers were also treated with a nitrogen-aniline plasma to generate polyaniline functional groups along the fiber surface, improving the chemical adhesion between fiber and matrix. The procedure used by Cruz *et al.* [16] was followed; the

fibers were placed in a reactor with nitrogen atmosphere operating under 80 W of power, 15 MHz, and 93.32 Pa of system pressure for 60 min. Subsequently, a second plasma treatment with an aniline atmosphere was applied for 90 min in the same reactor with the same operations conditions. Finally, these plasma-treated (PT) fibers were washed with xylene. The tensile properties of PT fibers were obtained as described in Section 2.2.

2.3.1 Infrared spectroscopy

Infrared (IR) spectroscopy was used to identify the difference in the chemical composition of the surface of UT and PT fibers. A Nicolet Protege 460 spectrophotometer was used to obtain the IR spectra. The pressed disk method was used to prepare pastille samples for the spectrophotometer. Pastilles were prepared by grinding up the UT fibers and mixing them with potassium bromide (KBr), using a sample/KBr ratio of 0.5/100 by weight. The same procedure was used to obtain the pastilles for PT fibers; however, only material from the fiber surface was used.

2.3.2 Scanning electron microscopy (SEM)

Surface examination of treated and untreated fibers was performed using a scanning electron microscope Jeol model JSM-6360LV.

2.4 Polariscope

A circular polariscope was used to determine the stress field in the epoxy matrix. The dark-field polariscope uses two polarizer plates with their polarization axis crossed at 90°, and two quarter-wave plates set at ±45° from the polarization axis of the first polarization plate which was set in a vertical orientation. The light-field polariscope was obtained by rotating the optical axis of the second polarizer plate to a vertical orientation. A sodium bulb was used as a light source (wavelength of 589 nm), resulting in an excellent-definition of the isochromatic fringes.

2.5 Photoelastic calibration of the epoxy resin

The photoelastic calibration of the epoxy resin was performed using the four-point bending method which produces stress patterns of pure bending. The stress-fringe coefficient of the material f_σ can be obtained using the following relationship,

$$f_\sigma = \frac{6Pay_N}{h^3 N} \tag{1}$$

where P is the applied load, a is the horizontal distance between the support and the loader (Fig. 1a), N is the fringe order, y_N is the distance from the neutral axis to the N^{th} fringe and h is the height of the beam (Fig. 1a).

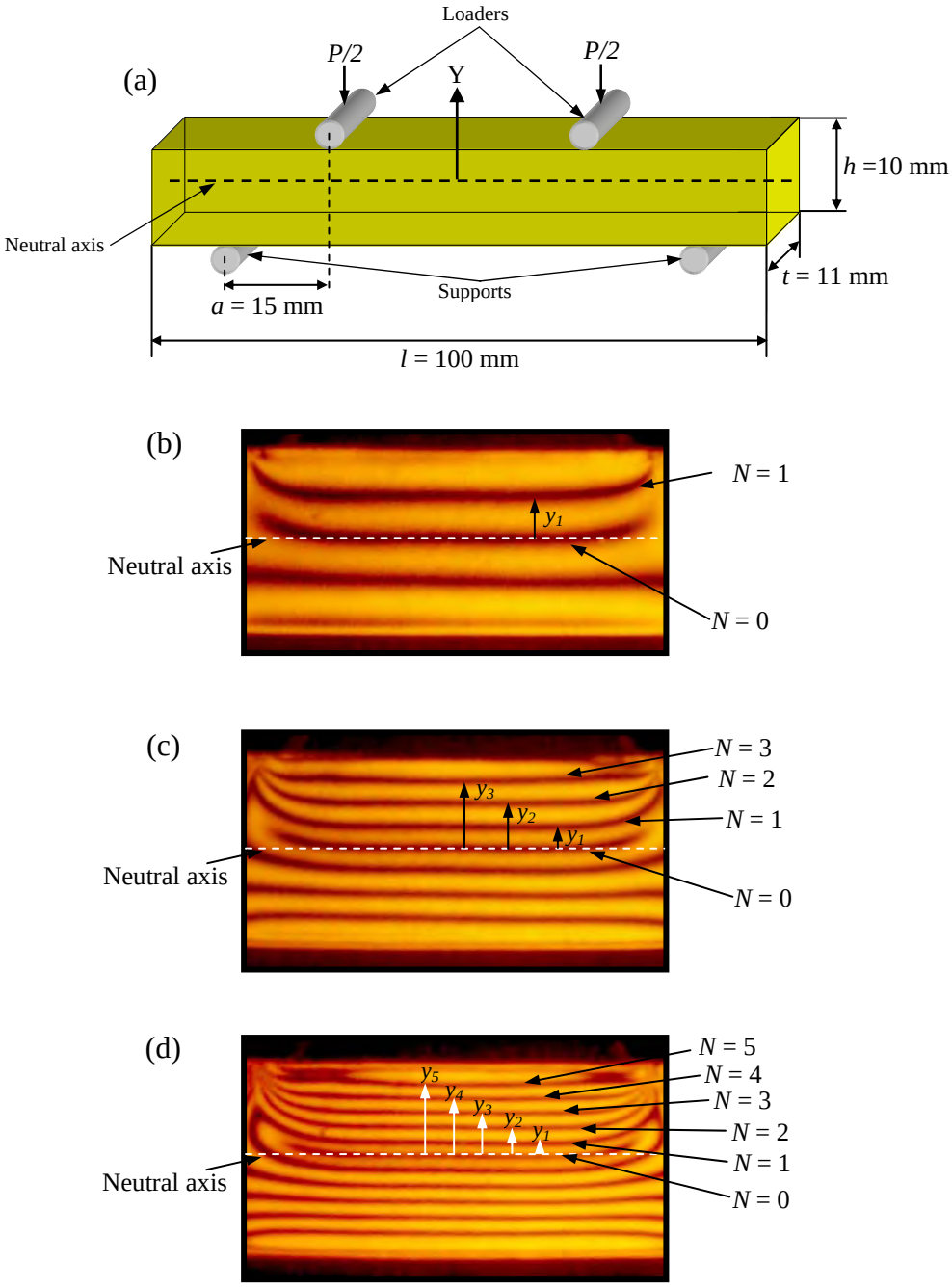

Figure 1. Isochromatic fringe patterns in epoxy resin four-point bending specimen: a) schematic, b) P = 30.67 N, (b) P = 61.31 N, (c) P = 91.97 N.

2.6 The pull-out test

2.6.1 Pull-out specimens

Model composites for pull-out testing were prepared using the epoxy resin and the fibers described in Sections 2.1 and 2.2, respectively. The dimension of the pull-out specimens are shown in Fig. 2.

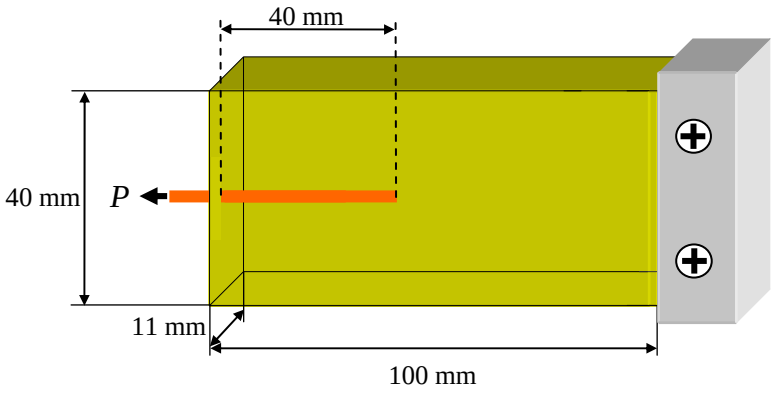

Figure 2. Pull-out specimen geometry.

2.6.2 Interfacial shear strength by photoelasticity

Pull-out tests were performed by clamping the resin block and loading the free end of the fiber in tension (Fig. 2). The dark- and light-field isochromatic photoelastic patterns along the fiber-matrix interface were recorded for several increments of load P. The applied load and interfacial shear stress patterns were monitored until the interface failed.

The interfacial shear stress at the interface τ_{max} was obtained following the procedure explained in Section 3.5. The interfacial shear stress τ_{max} was corrected using the relationship suggested by Schuster and Scala to obtain τ_{cmax} [17].

3. Results and discussion

3.1 Mechanical properties of the materials

Figure 3 shows typical stress-strain curves for UT, TX and PT fibers. It can be seen that all fibers have a similar behavior in the elastic regime. However, reductions in the failure stress of 10.6 and 6.8% were observed for TX and PT fibers, respectively, when compared to the UT fiber failure stress. These results indicate both fiber surface texturizing and plasma-treatment result in lower failure strength. It is believed, based on experimental observations, that the deformation of the fiber during pull-out tests occurs either entirely (for low-load cases) or mostly (for high-load cases) in the elastic regime; thus, the lower plastic properties of TX and PT fibers do not affect the analysis of the interface. Table 1 shows the mechanical properties of UT, TX and PT fibers obtained from Fig. 3.

The mechanical properties of the epoxy resin are: elastic modulus E=1032.05±50.85 MPa; tensile strength σ_0=22.76±1.84 MPa; and Poisson's ratio ν=0.38±0.01 [11].

Table 1. Mechanical properties of polyester fibers.

Material	Elastic modulus (MPa)	Tensile strength (MPa)	Failure stress (MPa)	Maximum strain (%)
TX fiber	5652.21±153.2	127.55±8.74	514.23±19.74	44.74±2.49
UT fiber	6003.61±252.4	139.38±9.65	568.64±1.71	46.62±2.60
PT fiber	6128.26±271.1	131.45±12.78	532.28±14.33	47.89±3.52

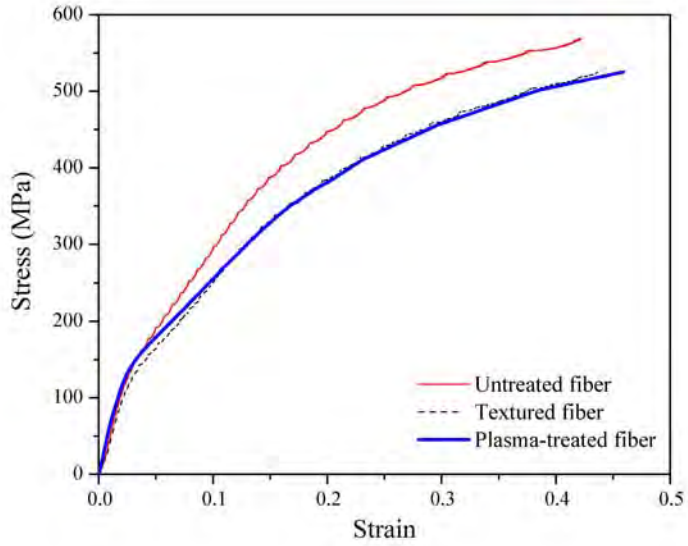

Figure 3. Typical stress-strain curves of untreated (UT), textured (TX) and plasma-treated (PT) fibers.

3.2 IR spectra of fibers

Figures 4a and 4b show the IR spectra for the UT and PT fibers, respectively. A difference in the chemical composition of the fiber surfaces can be observed: the spectrum in Figure 4b shows bands at 3380 and 1610 cm^{-1} corresponding to the N-H vibration and deformation, and also a band at 2940 cm^{-1} belonging to the C-H aliphatic vibration; these bands are characteristic of the polyaniline polymerization by plasma treatment [16], demonstrating that a layer of polyaniline was created on the surface of the fiber during the treatment.

3.3 Scanning electron microscopy (SEM)

Figures 5a and 5b show UT and TX fibers, respectively; Figure 5c shows a close-up view of the TX fiber surface. It can be seen that the striations of TX fiber are homogenous and orientated at 45° approximately with respect to the axial direction of the fiber. Each striation has a depth of approximately 100 μm. Figure 5d shows the SM fiber; it can be seen that the surface presents a pattern parallel to the fiber axial direction caused by sanding of the surface.

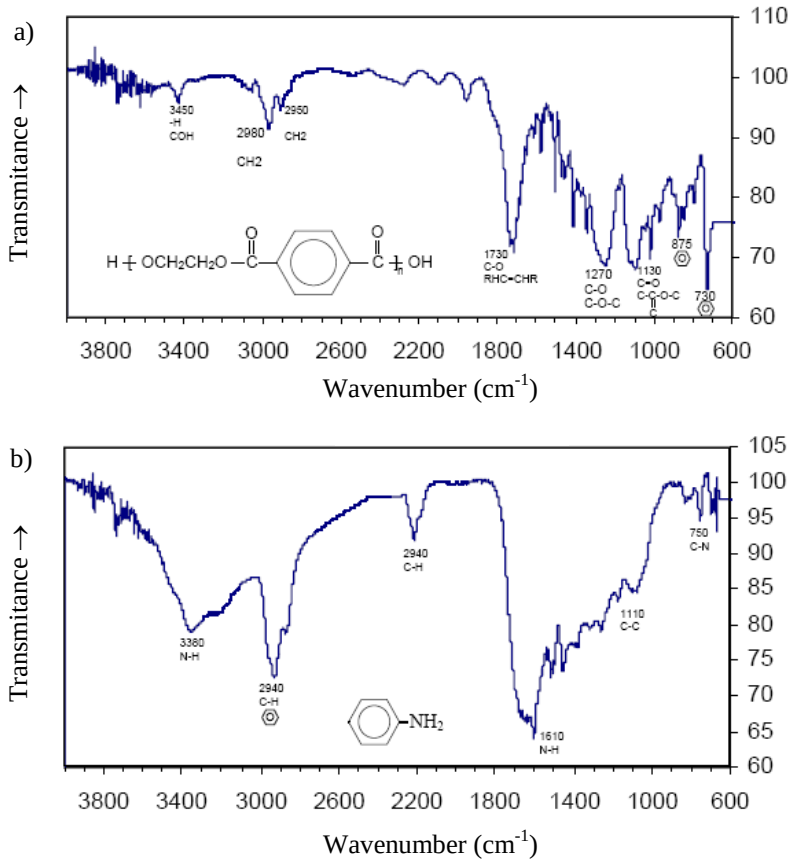

Figure 4. Infrared spectra of the surface of polyester fibers: a) UT fiber, b) PT fiber.

Figures 5e and 5f show the PT fiber before and after being washed with xylene, respectively. It can be observed in Fig. 5e that a thin layer of polyaniline was formed on the fiber surface after the plasma treatment; however, this layer was very brittle and was not bonded to the fiber. After the fiber was washed, a difference in the surface morphology is revealed, which may be attributed to the formation of polyanilyne bonded to the surface. Polyaniline was confirmed with the IR analysis in Section 3.2.

3.4 Photoelastic calibration of the epoxy resin

Figures 1(b-d) show the dark-field isochromatic fringe patterns in an epoxy resin beam at different applied loads. An increase in shear stress during four-point bending is indicated by an increase of the number of fringes (fringe order N) with the applied load. The stress-fringe coefficient was calculated using Eq.(1) by measuring the vertical distance y_N from the neutral axis to the N^{th} fringe at a specific applied load P. The average stress-fringe coefficient was calculated as f_σ=11114.10 N/m.

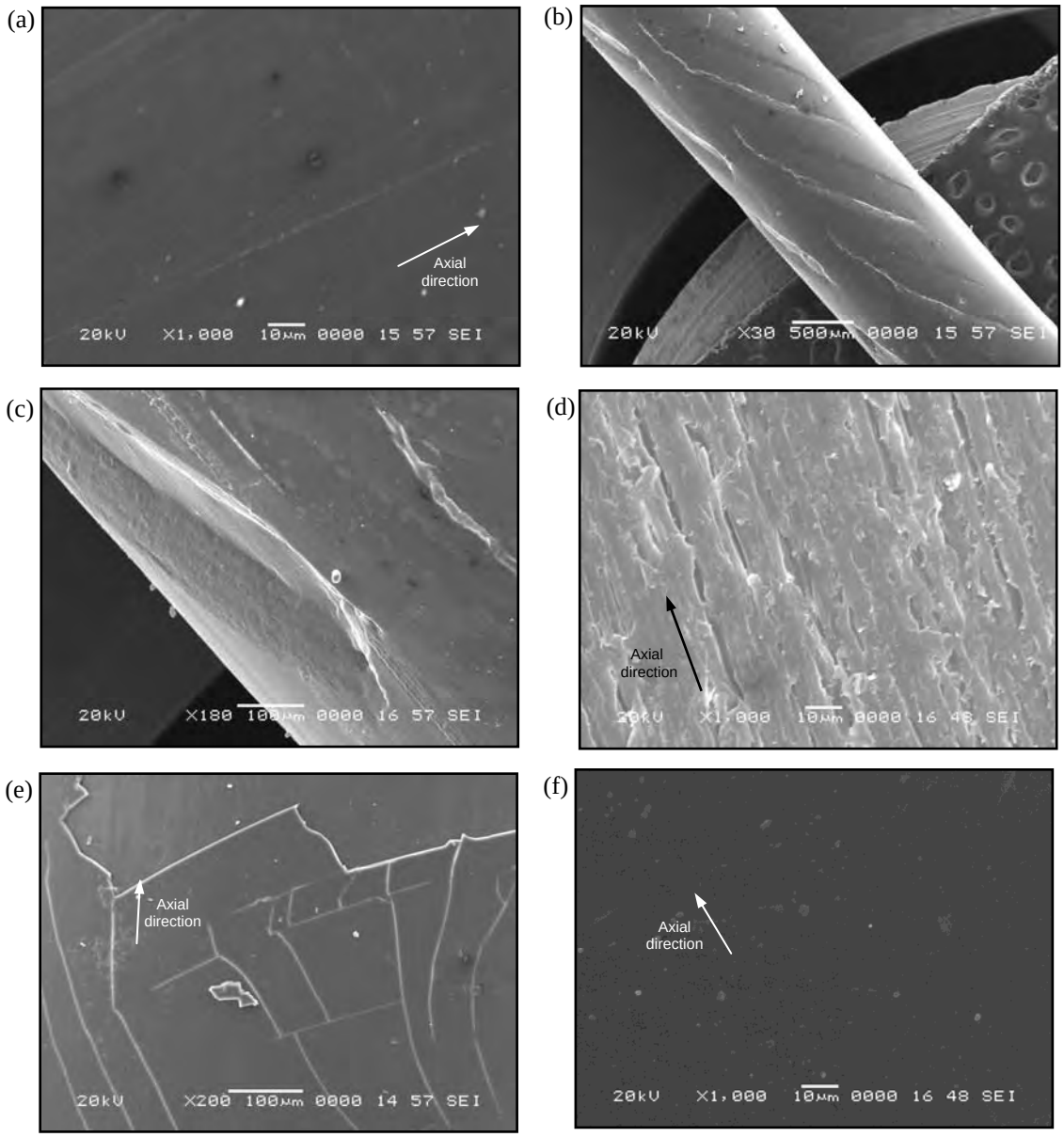

Figure 5. SEM micrographs of polyester fibers: a) untreated (UT) fiber, b) textured (TX) fiber, c) close-up view of TX fiber, d) surface-modified (SM) fiber, e) plasma-treated (PT) fiber, (f) Washed PT fiber.

3.5 Interfacial shear strength by photoelasticity

Figure 6 shows the dark-field isochromatic fringe patterns in the matrix of the SM fiber specimen at different applied loads. It can be seen that the fringe order *N* increases with the applied load, indicating an increase in the stress transfer to the matrix through the interface. To measure the interfacial shear strength of the model composite, the isochromatic fringe patterns from photographs recorded during the pull-out test were analyzed as outlined below.

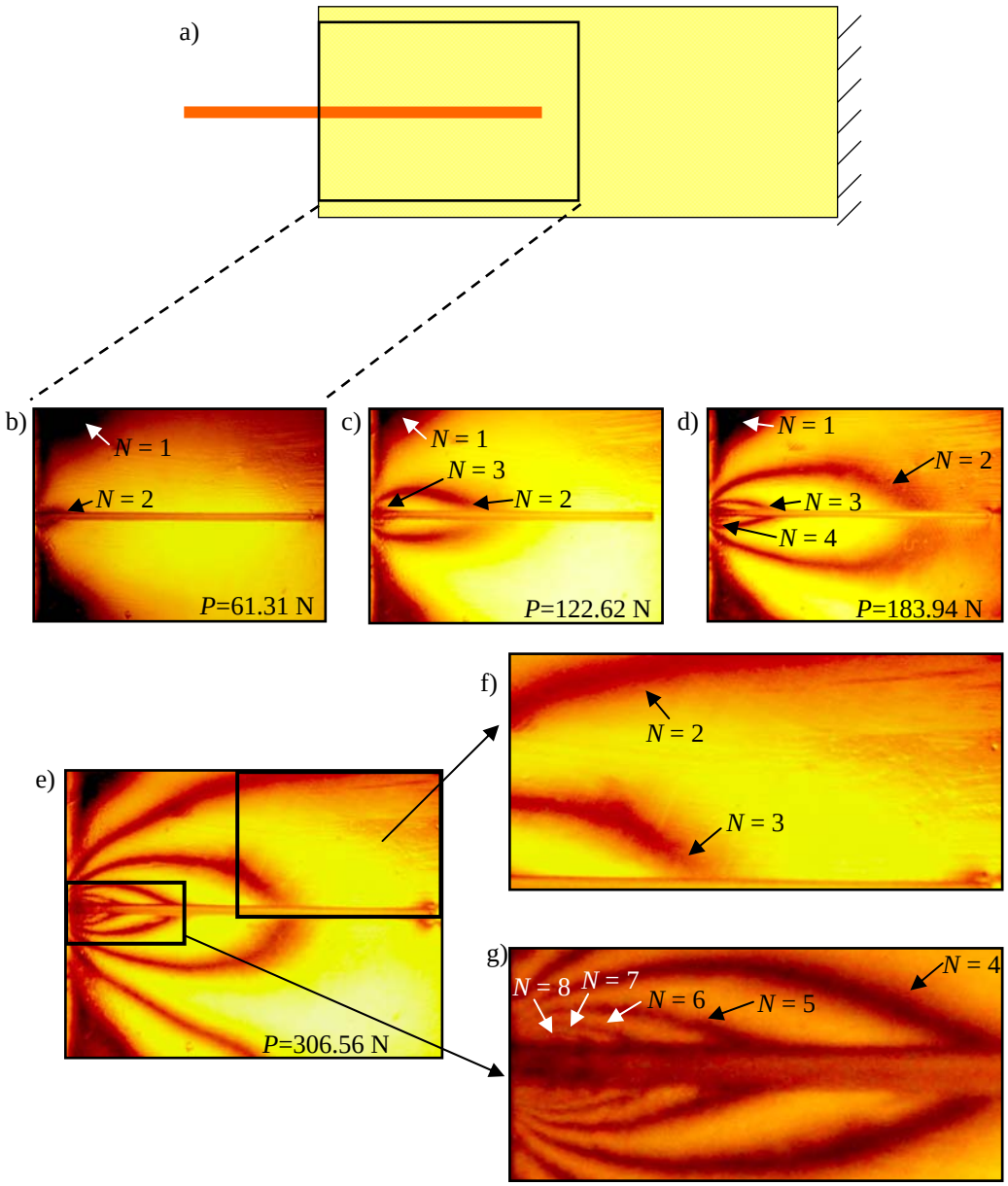

Figure 6. Isochromatic fringe patterns in SM fiber specimen.

A reference axis aligned with the edge of the specimen resin block was set, as shown in Figure 7a. Since the light intensity used offsets the observed location of the fringe edges from their actual locations, the actual distance to the right edge of the N^{th} fringe, x_N (Fig. 8), was calculated using the following proposed relationship,

$$x_N = x^R_N + (x^R_N - x^L_N) \quad (2)$$

where x^L_N and x^R_N are the observed intersection of the left and right edges of the N^{th} fringe, respectively, with the fiber (Fig. 8). The calculation of x_N in Eq.(2) is proposed

based on the observed photoelastic patterns in a single glass fiber/epoxy matrix composite [9, 18], where the actual intersection between the fringe and the fiber is located approximately one fringe thickness away from the apparent intersection.

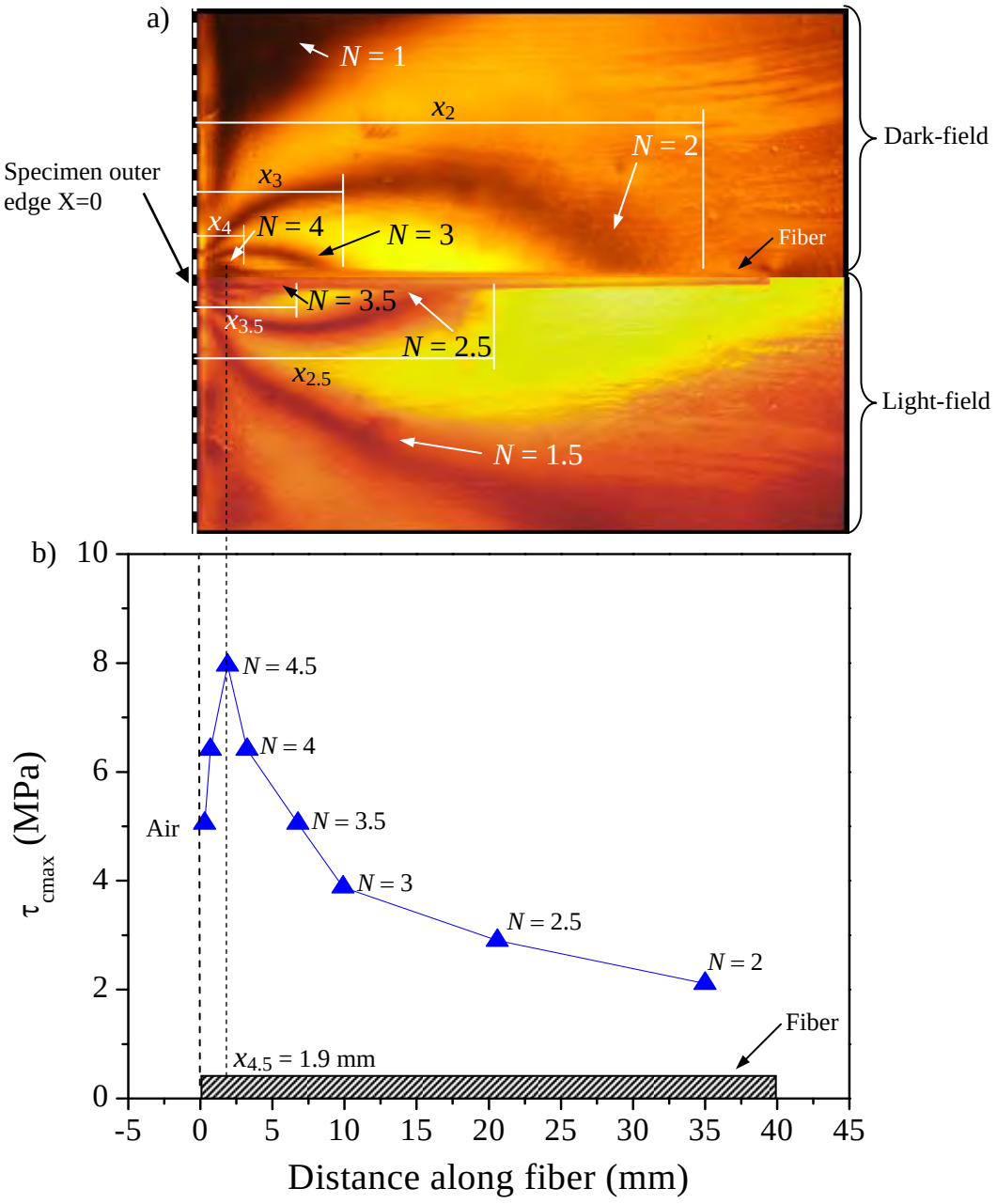

Figure 7. Determination of the shear stress distribution from isochromatic fringes in SM fiber specimen:
a) Isochromatic fringes for dark- and light field at *P*=183.94 N;
b) Distribution of the interfacial shear strength along the fiber.

It is noted that Figure 7a is made with images from both dark-field (upper part) and light-field (lower part) fringe patterns which correspond to the SM fiber specimen at P=183.94 N (Fig. 6d). The corresponding corrected interfacial shear strength τ_{cmax} of each fringe order N (Table 2) was plotted against its corresponding distance from the block edge of the specimen, as shown in Figure 7b.

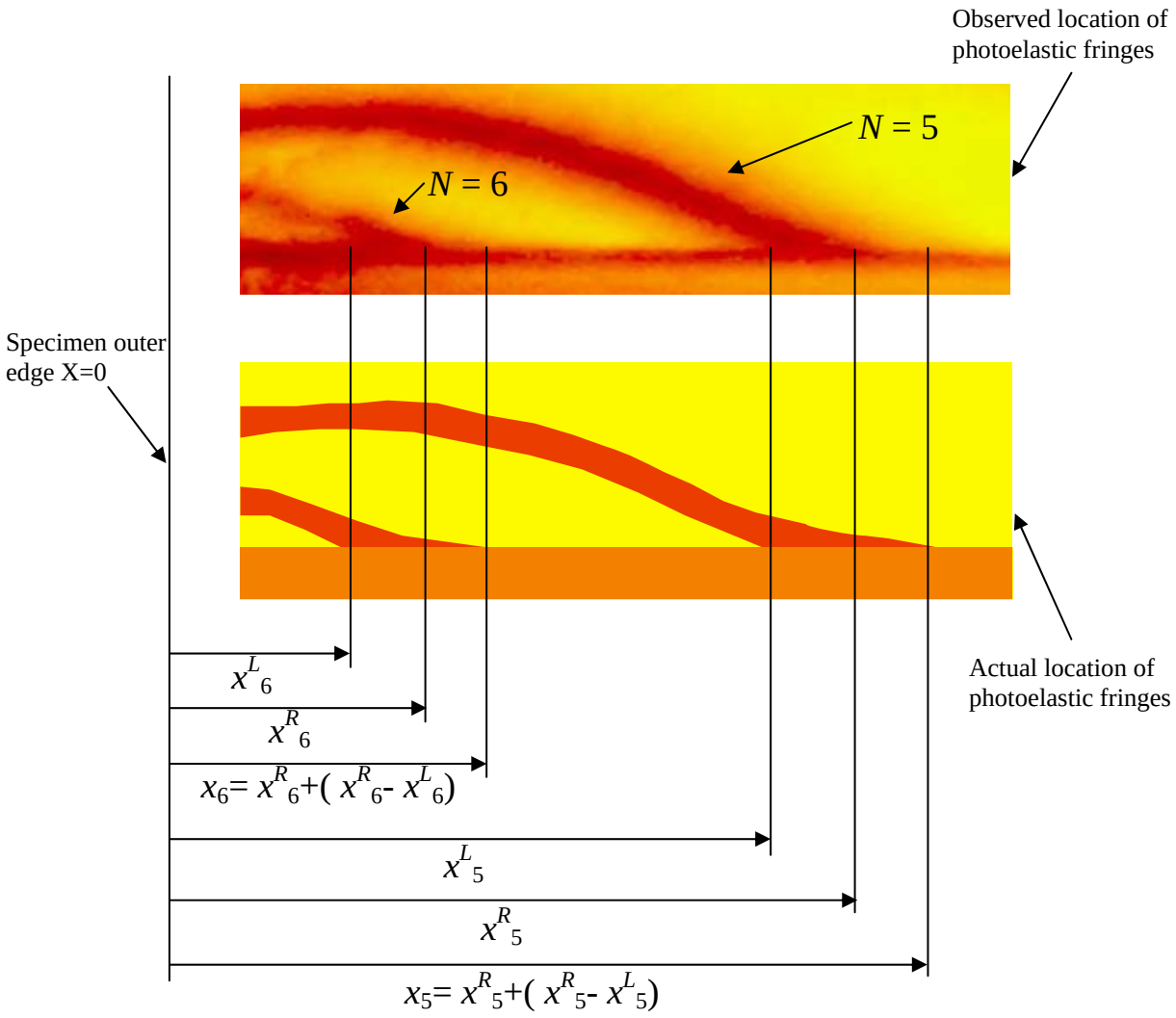

Figure 8. Calculation of x_N.

Table 2. Corrected shear stresses.

N	τ_{cmax} (MPa)
0.5	0.88
1.0	1.10
1.5	1.51
2.0	2.11
2.5	2.90
3.0	3.88
3.5	5.05
4.0	6.41
4.5	7.96
5.0	9.70
5.5	11.62
6.0	13.74
6.5	16.05
7.0	18.55
7.5	21.24
8.0	24.12

Figure 9 shows the profile of the normalized interfacial shear stress τ_{cmax}/σ_n (where σ_n is the applied stress to the free end of the fiber) *versus* the fiber aspect ratio L/D (where L is the embedded length) for the different surface-treated fibers. It can be seen that τ_{cmax}/σ_n reaches a maximum along the fiber at a point located near the specimen outer edge (L/D<5). It is possible that some debonding may have occurred prior to loading at a point near where the fiber enters the specimen resin block. After reaching a maximum, τ_{cmax}/σ_n decays along the interface; however, the trend of the curves shows that τ_{cmax}/σ_n will not reach zero at the end of the embedded fiber as predicted by shear–lag model (Fig. 10). This can be seen in Fig. 6f, where the photoelastic fringe patterns at the end of the embedded fiber are observed. A possible explanation for this observation could be that both the fiber and matrix do not have an entirely linear elastic behavior at high load and consequently some permanent deformation is present; however, further research must be carried out to confirm this assumption.

It can also be observed from Figure 9 that the location of the τ_{cmax}/σ_n moves towards the fiber end with the applied load. This is caused by incremental debonding of the embedded fiber surface as the applied load on the free fiber is increased. As the load applied to the free fiber is increased from 61.31 to 183.94 N, the position of τ_{cmax}/σ_n along the embedded fiber moved 0.7 and 0.6 times the fiber diameter for UT and TX fibers, respectively, while it only moved 0.08 times the fiber diameter for both SM and PT fibers. This improvement is caused by the increase of the interfacial strength of treated fiber/epoxy systems.

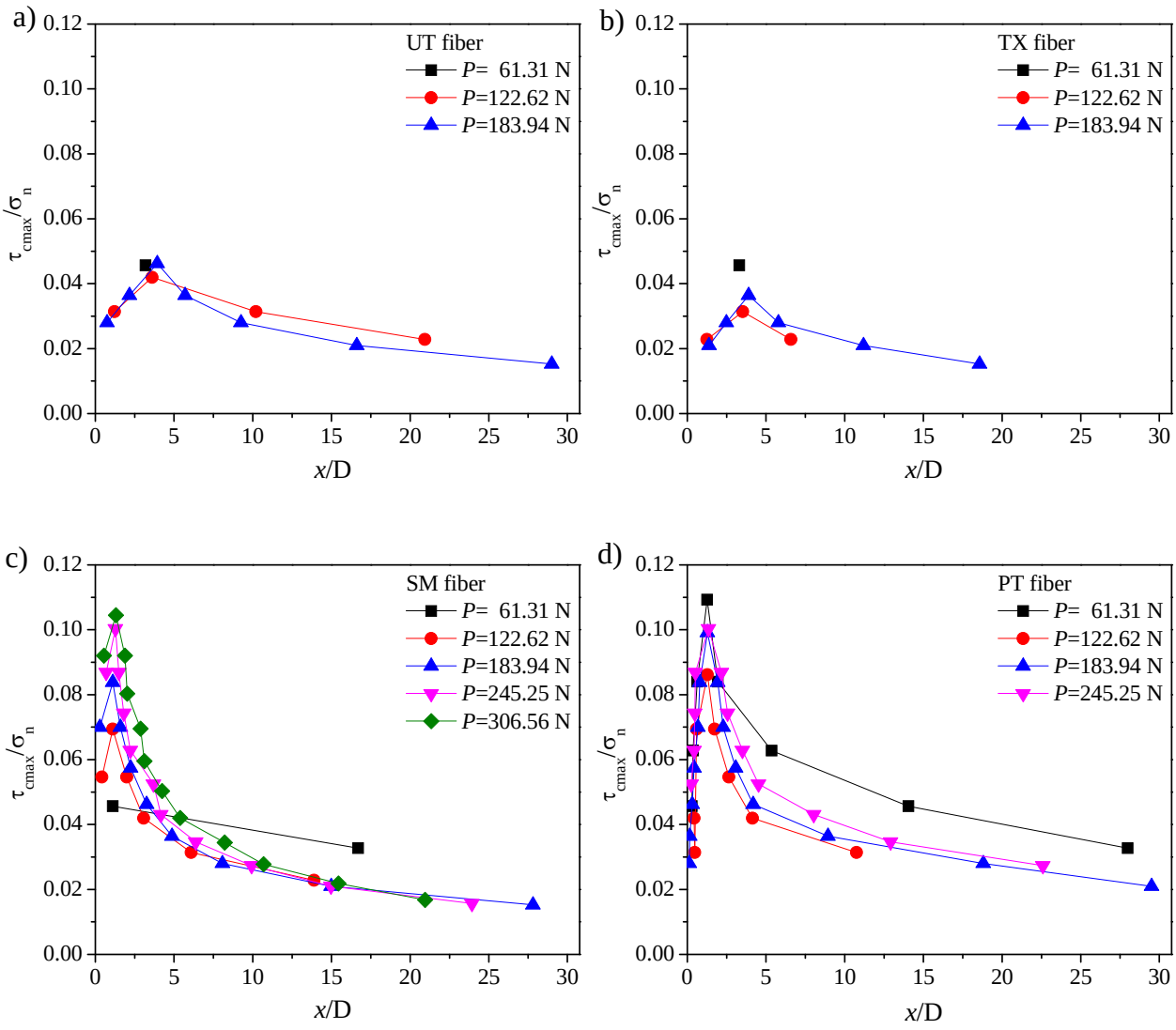

Figure 9. Distribution of the normalized interfacial shear strength along the interface of polyester/epoxy composites: a) UT fiber, b) TX fiber, c) SM fiber, PT fiber.

The maximum applied load to the pull-out fiber specimens increased 33.33 % and 66.66 % for PT and SM fibers, respectively, when compared to UT and TX fibers (Fig. 9). Consequently, the improved interface transferred more load to the matrix before debonding.

It is noted that the performance of the TX fibers was lower than the UT fibers. It is believed that the size of the striations produced a non-continuous interfacial contact between the fiber and the matrix rather than an interlocking resulting in a poor bonding condition.

If the τ_{cmax}/σ_n profiles are compared for the same applied load on the free fiber (P = 183.94 N), increases of 115 % and 83 % are observed for PT and SM fibers, respectively, when compared to the UT fiber (Fig. 10). This trend also shows the

improvement of the stress transfer to the matrix due to a better interface. The shear-lag model was also fit to the experimental data as shown in Fig. 10. The following relation for pull-out was used [2],

$$\frac{\tau}{\sigma_n} = \frac{n}{2}\left[\frac{\cosh\left(\frac{n(L-x)}{r}\right)}{\sinh\left(\frac{nL}{r}\right)}\right] \tag{3}$$

where τ is the interfacial shear stress, n is the shear-lag parameter, x is position along the fiber surface and r is the fiber radius. By varying the shear-lag parameter n, it was possible to fit the shear-lag model to the experimental data. The ratio n/n_{ref} for the fit shear-lag model is shown in Fig. 10, where n_{ref} is the shear-lag parameter for the UT fiber. It can be seen that the surface modifications improve the interfacial adhesion while the performance of the TX fiber is decreased when compared with the UT fiber.

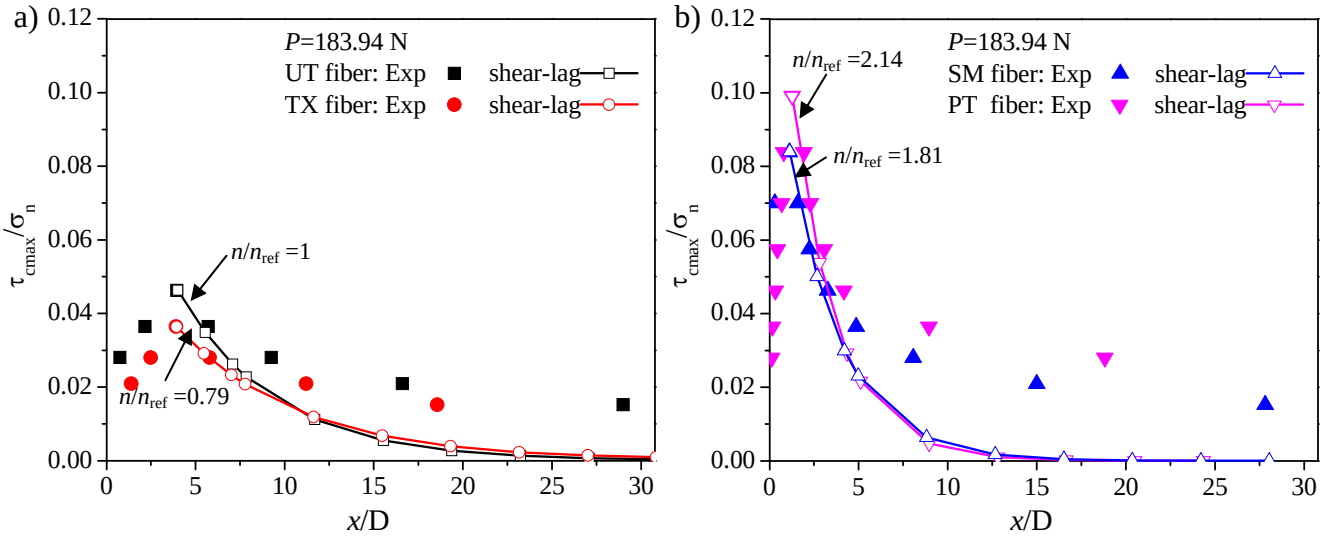

Figure 10. Comparison between shear-lag model and the distribution of the normalized interfacial shear strength along the interface of polyester/epoxy composites for a load of P=183.94 N: a) UT and TX fibers, b) SM and PT fibers.

4. CONCLUSIONS

The effect of surface modification on the polyester fiber/epoxy model composite was studied using pull-out test and photoelasticity. It was found that nitrogen-aniline plasma treatment and mechanical surface modification improved the interfacial adhesion. These treatments allow the composite to perform better by carrying a higher

load prior to interfacial failure, due to an increase of fiber-matrix stress transfer with reduced debonding at higher loads.

ACKNOWLEDGEMENTS

This work was supported by the Consejo Nacional de Ciencia y Tecnología (CONACYT), México, Project J-28642U. The authors would like to thank Dr. R. Olayo from the Universidad Autónoma Metropolitana for performing the plasma treatment of the fibers, and C. Martín-Barrera from the Centro de Investigación Científica de Yucatán for performing the uniaxial tensile tests.

REFERENCES

1. Shaker M, Kamel I, Ko F, Song JW. Improvement of the interfacial adhesion between Kevlar fiber and resin by using R-F plasma. J Compos Tech Res 1996;18(4):249-255.
2. Gonzalez-Chi PI, Young RJ. Deformation micromechanics of a thermoplastic-thermoset interphase of epoxy composites reinforced with poliethylene fiber. J Mater Sci 2004;39(23):7049-7059.
3. Wu GM, Shyng YT, Kung SF, Wu CF. Oxygen plasma processing and improved interfacial adhesion in PBO fiber reinforced epoxy composites. Vacuum 2009;83(Supplement 1):S271-S274.
4. Valadez-Gonzalez A, Cervantes-Uc JM, Olayo R, Herrera-Franco PJ. Effect of fiber surface treatment on the fiber-matrix bond strength of natural fiber reinforced composites. Compos Part B-Eng 1999;30(3):309-320.
5. Kalantar J, Drzal LT. The bonding mechanism of aramid fibres to epoxy matrices. J Mater Sci 1990;25(10):4186-4193.
6. Sreekumar PA, Thomas SP, Saiter Jm, Joseph K, Unnikrishnan G, Thomas S. Effect of fiber surface modification on the mechanical and water absorption characteristics of sisal/polyester composites fabricated by resin transfer molding. Compos Part A-Appl S 2009;40(11):1777-1784.
7. Ou R, Zhao H, Sui S, Song Y, Wang Q. Reinforcing effects of Kevlar fiber on the mechanical properties of wood-flour/high-density-polyethylene composites. Compos Part A-Appl S 2010;41(9):1272-1278.
8. Chua PS, Piggott MR. The glass fibre--polymer interface: I--theoretical consideration for single fibre pull-out tests. Compos Sci Technol 1985;22(1):33-42.
9. Herrera-Franco PJ, Drzal LT. Comparison of methods for the measurement of fibre/matrix adhesion in composites. Compos 1992;23(1):2-27.
10. Mäder E, Melcher S, Liu J, Gao S, Bianchi A, Zherlitsyn S, Wosnitza J. Adhesion of PBO fiber in epoxy composites. J Mater Sci 2007;42(19):8047-8052.
11. Vázquez-Rodríguez JM, Herrera-Franco PJ, González-Chi PI. Analysis of the

interface between a thermoplastic fiber and a thermosetting matrix using photoelasticity. Compos Part A-Appl S 2007;38(3):819-827.
12. Ramirez FA, Carlsson LA, Acha BA. A method to measure fracture toughness of the fiber/matrix interface using the single-fiber fragmentation test. Compos Part A-Appl S 2009;40(6-7):679-686.
13. Tyson WR, Davies GJ. A photoelastic study of the shear stresses associated with the transfer of stress during fibre reinforcement. Br J Appl Phys 1965;16(2):199-205.
14. Zhao FM, Hayes SA, Patterson EA, Jones FR. Phase-stepping photoelasticity for the measurement of interfacial shear stress in single fibre composites. Compos Part A-Appl S 2006;37(2):216-221.
15. Zhao FM, Liu Z, Jones FR. Photoelastic determination of interfacial shear stresses in model composites. Key Eng Mat 2007;334-335:289-292.
16. Cruz GJ, Morales J, Castillo-Ortega MM, Olayo R. Synthesis of polyaniline films by plasma polymerization. Synthetic Met 1997;88(3):213-218.
17. Schuster DM, Scala E. The mechanical interaction of sapphire whiskers with a birefringent matrix. Trans Metall Soc AIME 1964;230:1635-1640.
18. Cloud G. Optical Methods in Experimental Mechanics Part 3: Path Length and the Generic Interferometer. Exp Techniques 2002;26(5):13-15.